ONLINE FIRST

This is a provisional PDF only. Copyedited and fully formatted versión will be made available at final publication

HISTOLOGY AND HISTOPATHOLOGY

ISSN: 0213-3911
e-ISSN: 1699-5848

Moringa isothiocyanate-1 mitigates the damage of oxidative stress and apoptosis in diabetic nephropathy mice

Authors: Zhou Hua, Jiuhong Deng and Guiying Wang

DOI: 10.14670/HH-18-741
Article type: ORIGINAL ARTICLE
Accepted: 2024-04-03
Epub ahead of print: 2024-04-03

Moringa isothiocyanate-1 mitigates the damage of oxidative stress and apoptosis in diabetic nephropathy mice

Zhou Hua[1], Jiuhong Deng[2], Guiying Wang[3*]

[1] Department of Nephrology, The People's Hospital of Suichang County, Lishui City 323300, Zhejiang Province China

[2] Department of Endocrinology, Second People's Hospital of Pingyang County, Wenzhou City 325405, Zhejiang Province, China

[3] Department of Nephrology, Shangyu People's Hospital of Shaoxing, Shaoxing City 312300, Zhejiang Province, China

Corresponding author: Guiying Wang, E-mail: wgy8320@163.com

Running title: MIC-1 mitigates the nephropathy of diabetic mice

Abstract

Objective: Diabetic nephropathy (DN) is a prevalent cause of end-stage kidney disease worldwide. Moringa isothiocyanate-1 (MIC-1) has shown potential for DN management, however, the exact mechanisms remain unclear. This research intended to evaluate the impact and mechanism of MIC-1 on DN.

Methods: Six C57BLKS/J-db/m mice served as controls. Eighteen C57BLKS/J-db/db mice were randomly separated into three groups: db/db, db/db + irbesartan (IBS), and db/db + MIC-1. Three weeks post-drug administration, the body weight and kidney weight of mice in each group were measured. Concurrently, serum creatinine (Scr), urine albumin, insulin, glycosylated hemoglobin (GHb), oxidative stress-, and inflammatory-related factors were determined. Additionally, the pathological injury, apoptosis, apoptosis-related markers, NLRP3, and ASC levels in the kidney tissues were examined utilizing H&E, Masson, PAS, TUNEL staining, and Western blot.

Results: MIC-1 decreased the body weight, kidney weight, the levels of Glu, Scr, and urine albumin in db/db mice. Moreover, MIC-1 significantly suppressed the levels of MDA, insulin, GHb, TNF-α, IL-1β, and IL-6, while increased the activities of SOD, CAT, and GPX in the serum of db/db mice. MIC-1 also mitigated the kidney tissue injury in db/db mice. Western blot assay showed that MIC-1 enhanced the Bcl-2 level and suppressed the Bax, cleaved caspase-3, cleaved caspase-9, NLRP3, ASC, and caspase-1 levels of the kidney tissues in db/db mice.

Conclusions: MIC-1 ameliorated the kidney injury in DN mice, and its mechanism may be associated with the suppression of renal cell apoptosis, oxidative stress, and inflammatory responses.

Keywords: diabetic nephropathy; moringa isothiocyanate-1; oxidative stress; apoptosis

Introduction

Diabetic nephropathy (DN) is a disease with distinctive pathological structure and function changes engendered by diabetes, and it has grown to be the foremost cause of end-stage kidney disease (ESKD) (VR et al. 2019). In China, the incidence and prevalence of DN have increased dramatically over the past decade (Samsu 2021). By 2040, the global population of diabetes is estimated to elevate to 642 million, of which 30%-40% will develop to DN (Tang and Yiu 2020). The primary clinical characteristics of DN are renal lesions, such as edema, proteinuria, hypertension, and renal insufficiency, which are the major reasons responsible for ESKD and renal failure (Ioannou 2017). At present, conventional therapies for DN mainly focus on blood glucose control, blood pressure moderation, repression of the renin-angiotensin system, and renal transplantation (Yamazaki et al. 2021). However, these interventions do not prevent the progression of chronic kidney disease (CKD) in the majority of patients with DN. Hence, discovering anti-DN medicaments with low toxicity and profound efficacy has emerging as a novel hot spot in the management of DN.

In recent years, the theoretical and clinical exploration of traditional Chinese medicine (TCM) in treating DN has made continuous progress, exhibiting unique advantages in alleviating oxidative stress, reducing inflammatory response, and ameliorating podocyte injury (Ma et al. 2021; Ou et al. 2021). *Moringa Oleifera* Lam., a perennial tropical tree of the Moringaceae, has high economic and medicinal value. *Moringa Oleifera* seeds (MOS) are rich in diverse bioactive ingredients, which are beneficial for human health (Araújo et al. 2013; Wen et al. 2022; Fakurazi, Hairuszah, and Nanthini 2008). MOS contained isothiocyanate derivatives with biological activities such as anti-inflammatory, anti-oxidative, anti-bacterial, and anti-diabetic (Sailaja et al. 2021; Padla et al. 2012; Kou et al. 2018). Of these, Moringa isothiocyanate-1 (MIC-1) is the main isothiocyanate (Sailaja et al. 2021). A study has clarified that MOS extracts alleviated oxidative stress injury and renal fibrosis by activating GSK-3β and Nrf2/HO-1 pathways, thereby protecting renal function (Wen et al. 2022). Waterman C et al. reported that MIC-enriched seed extract postponed the onset of diabetes in type-2 diabetes rats (Waterman et al. 2020). Some scholars have illustrated that MIC-1 reversed epigenome and transcriptome changes in mouse renal mesangial cells mediated by high glucose (Li et al. 2019). In addition, numerous studies have demonstrated that MIC-1 could alleviate inflammation, apoptosis, and oxidative processes closely related to human diseases, including DN (Kim et al. 2017; Giacoppo et al. 2017; Xie et al. 2021). Nonetheless, it remains unclear whether

MIC-1 can retard DN progression by restraining apoptosis, inflammation, and oxidative stress. Therefore, in this study, db/db mice were selected as the research subjects to explore the effect of MIC-1 on renal function and pathological damage, apoptosis, inflammation, and oxidative stress in db/db mice, to offer a scientific foundation for the TCM therapy of DN.

Materials and methods

Experimental animals

Shanghai SLAC Laboratory Animal Co., Ltd offered male C57BLKS/J db/m mice (n=6, 8-week-old) and C57BLKS/J db/db mice (n=18, 8-week-old). These animals underwent a seven-day acclimatization, aligning with standard norms encompassing temperature (25 ± 2℃), relative humidity (55 ± 5%), and illumination (12-hour segregation between day and night cycles).

Experimental design

Irbesartan (IBS, I129263) was bought from Aladdin (China). MIC-1 was extracted from *Moringa Oleifera* seeds referring previous report (Xie et al. 2021). Six db/m mice served as controls. Eighteen db/db mice were randomized into the db/db, db/db + IBS, and db/db + MIC-1 groups, with six mice in each group. The mice in the db/db + IBS group were subjected to IBS by gastric lavage at a dose of 50 mg/kg/d in 10% DMSO for 21 days (Deng, Cheng, and Shen 2016). The mice in the db/db + MIC-1 group were treated with MIC-1 by gastric lavage at a dose of 100 mg/kg/d in 10% DMSO for 21 days (Kim et al. 2018). The dosage was adjusted weekly to accommodate changes in body weight during the study period. The mice in the db/m and db/db groups were given excipient solution in the same way. The design of the study is presented in Figure 1A. Blood glucose (Glu) levels were assessed by a blood glucose meter (580, Yuwell, China) every two weeks. After 21 consecutive days of drug treatment, each mouse was placed in a metabolic cage to harvest a 24-hour urine for analysis. The body weight of the mice in each group was measured. A liquid protein extraction reagent was applied to obtain urine albumin (P1255, Applygen, China). Next, a BCA kit (P1513, Applygen, China) was exploited to quantify the extracted urine albumin.

Sample collection

Upon completion of the 21-day treatment, mice were anesthetized with 2% isoflurane (R510-22, RWD Life Science Co., China), and blood samples were collected from the eyes. All blood samples were centrifuged (4℃, 1000 g, 20 min) and serum was obtained. After that, mice were euthanized by CO_2, and kidneys were quickly harvested and weighed. Then the kidney-to-body weight ratio was calculated according to the formula: 100*kidney weight/body weight. Part of the kidney samples was fixed via 4% paraformaldehyde (PFA, G1101, Servicebio, China), dehydrated, paraffin-embedded, sliced (4 μm), and the remainder stored at -80℃ for future analysis

Measurement of renal function

Serum creatinine (Scr) was estimated utilizing an automatic biochemical analyzer (AU680, Beckman, USA), and glycosylated hemoglobin (GHb) content was estimated utilizing another automated GHb analyzer (Variant II, BIO-RAD, USA). Serum insulin was assessed by the ELISA method utilizing the Mouse Ins1 / Insulin-1 ELISA Kit (RAB0817, Sigma-Aldrich, USA).

Determination of oxidative stress-associated biomarkers

In brief, lysate (P0013, Beyotime, China) was added to the kidney samples and then homogenized. The proportion of tissue weight to lysate was 10%. After centrifugation, the supernatant was harvested. Then, the contents of MDA, SOD, CAT, and GPX were examined utilizing the MDA (S0131M, Beyotime, China), SOD (S0109, Beyotime, China), CAT (S0051, Beyotime, China), and GPX assay kits (S0056, Beyotime, China), separately.

Kidney histopathological analysis

Servicebio (China) offered the Hematoxylin and Eosin (H&E) (G1003), Masson (G1006), and Periodic Acid-Schiff (PAS) kits (G1008). After being routinely dewaxed utilizing xylene and then hydrated utilizing gradient ethanol, the kidney slices were stained with the H&E, Masson, and PAS kits, respectively. After rinsing, slices were dehydrated and permeabilized. Thereafter, neutral resin (abs9177, Absin, China) was exploited to block the slices. Lastly, the pathological damage and degree of fibrosis of kidney tissues were captured using an optical microscope (BX53M, Olympus, Japan).

TUNEL assay

The TUNEL kit (C1090, Beyotime, China) was employed to assess the apoptosis of kidney tissues. The proteinase K solution (P1120, Solarbio, China) was added to the dewaxed and hydrated slices at room temperature for 20 min. After rinsing, the prepared TUNEL solution was applied to treat the slices at RT for 60 min. After that, a DAPI solution (C1005, Beyotime, China) was added. After being dehydrated and transparentized, the slices were subjected to neutral resin. Apoptosis of the kidney tissues was observed utilizing an optical microscope (Nikon Eclipse Ci-L, Nikon, Japan).

Detection of inflammation-related factors

Meimian (China) provided the TNF-α (MM-0132M1), IL-1β (MM-0040M1), and IL-6 kits (MM-0163M1). The contents of TNF-α, IL-1β, and IL-6 in serum samples were estimated in strict accordance with the corresponding instructions of the TNF-α, IL-1β, and IL-6 kits by ELISA assay.

Western blot analysis

Total protein from the kidney tissues was lysed with lysis buffer (abs9229, Absin, China). After being quantified with the help of a BCA kit (G2026, Servicebio, China), protein samples were subjected to denaturation and electrophoresis and then blotted onto nitrocellulose membranes. They were subsequently sealed with 5% non-fat milk at 37℃ for 90 min. After the blocked membranes were hybridized with primary antibodies at 4℃ overnight, the bound antibodies were then exposed to Goat Anti-Rabbit IgG (H+L) HRP (1:5000, S0001, Affinity) at 37℃ for 60 min. Thereafter, the membranes were examined with a gel imaging system (A44114, Invitrogen, USA) after being developed with a color reagent (E266188, Aladdin, China). The primary antibodies of Bcl-2 (1:2000, AF6139), Bax (1:8000, AF0120), cleaved caspase-3 (1:5000, AF7022), caspase-3 (1:2000, AF6311), ASC1 (1:5000, DF13176), NLRP3 (1:1000, DF7438), caspase-1 (1:1000, AF5418), pro-caspase-1 (1:1000, Ab179515), cleaved caspase-9 (1:2000, AF5240), caspase-9 (1:2000, AF6348) and β-actin (1:5000, AF7018) were bought from Affinity (USA).

Statistical analysis

Quantitative data were expressed as mean ± standard deviation. All experiments were conducted at least three times and SPSS software (16.0, IBM, USA) was utilized to process data. Statistical

analyses were conducted with the use of a one-way ANOVA for comparing differences among multiple groups. Comparison between groups was evaluated by the LSD test. The Kruskal-Wallis H test was deployed for heterogeneity of variance. P <0.05 represented statistical significance.

Results

MIC-1 attenuated the renal dysfunction of db/db mice

Assessing the general physical signs of the mice in each group, as exhibited in Figure 1B, the body weight, kidney weight, and kidney organ index in the db/db group were higher relative to the db/m group (P<0.01). Interestingly, IBS and MIC-1 clearly alleviated these basic indicators in db/db mice (Figure 1B, P<0.05). Moreover, we also noted that the levels of Glu, Scr, and urine albumin in db/db mice were upregulated, while were greatly decreased by IBS and MIC-1 intervention (Figure 1B, P<0.01).

MIC-1 suppressed the oxidative stress of db/db mice

Oxidative stress has been acknowledged as a considerable stimulator in DN development. In Figure 2A-2D, when compared with the db/m group, the level of MDA was elevated and the activities of SOD, CAT, and GPX were decreased in the db/db group (P<0.01). Importantly, IBS and MIC-1 notably decreased the MDA level and increased the activities of SOD, CAT, and GPX in serum of DN mice (Figure 2A-2D, P<0.01).

MIC-1 mitigated the kidney tissue injury of db/db mice

We utilized histological staining to observe the renal pathological changes in db/db mice. H&E staining results manifested that the kidney structure of db/db mice was severely damaged relative to db/m mice, characterized by severe cellular defects and blurred vascular striae (Figure 3). MIC-1 and IBS intervention alleviated the above renal histopathological injuries in db/db mice (Figure 3). Injury to the kidney tissue of db/db mice was also observed by Masson staining results, with a large number of fat vacuoles in the cytoplasm of cells and distinct blue fibrous tissue hyperplasia (Figure 3). Compared with the db/db group, the db/db + MIC-1 and db/db + IBS groups present less cell rupture and notably decreased blue fibrous tissue (Figure 3). PAS staining indicated a marked increase in the mucus secretion of kidney tissue in DN mice and the proliferation of

bronchial goblet cells, while MIC-1 and IBS intervention lessened these abnormal pathological injuries (Figure 3).

The contents of insulin and GHb in db/db mice were decreased by MIC-1

As illustrated in Figures 4A and 4B, the levels of insulin and GHb were highly increased in db/db mice (P<0.01). After intervened with MIC-1 and IBS, the levels of insulin and GHb were downregulated (P<0.01).

MIC-1 inhibited the cell apoptosis of kidney tissues of db/db mice

The apoptosis of kidney tissues was observed by the TUNEL assay. Compared with the db/m group, the apoptotic cell rate of the db/db group was significantly higher; compared with the db/db group, the percentage of apoptotic cells in db/db + MIC-1 and db/db + IBS mice decreased notably (Figure 5A, P<0.01). In addition, at the molecular level, significant downregulation of Bcl-2 protein and upregulation of Bax, cleaved caspase-3, and cleaved caspase-9 were observed in DN kidneys compared to db/m (Figure 5B, P<0.01). Treatment with MIC-1 or IBS restored the Bcl-2 protein level and consequently restrained the expressions of Bax, cleaved caspase-3, and cleaved caspase-9 proteins within db/db+IBS and db/db+MIC-1 groups (Figure 5B, P<0.05).

MIC-1 alleviated the inflammatory response of db/db mice

The increased levels of TNF-α, IL-1β, and IL-6 in DN mouse serum of the db/db group were detected than those in the db/m group (Figure 6A-6C, P<0.01). In contrast, after the intervention of IBS and MIC-1, the above inflammatory factors were significantly decreased (Figure 6A-6C, P<0.01).

MIC-1 inhibited the NLRP3, ASC, and caspase-1 levels of the kidney tissues in db/db mice

Western blot showed that the protein levels of NLRP3, ASC, and caspase-1 in the kidney of the db/db group were obviously higher than those of the db/m group (Figure 7A-7B, P<0.01). Remarkably, MIC-1 or IBS treatment decreased the expression of these proteins (Figure 7A-7B, P<0.05).

Discussion

MIC-1 has been exploited to treat various chronic diseases associated with inflammation, including diabetes. Waterman C et al. elucidated that MIC-1 intervention effectively delayed the onset of type 2 diabetes in a rat model (Waterman et al. 2020). In this study, we conducted animal experiments to evaluate the effect of MIC-1 on DN. Our results demonstrated that, after MIC-1 intervention, the body weight, kidney weight, and kidney organ index of db/db mice decreased notably. Then we assessed renal function indicators, as they can reflect the severity of DN to a large extent, especially Scr, a crucial indicator of renal function (Jin et al. 2019). Our study demonstrated that MIC-1 exhibits renal protective potential, evident as the reduction of Scr and urine albumin levels. In addition, the levels of blood glucose, insulin, and GHb are generally considered to be the primary indicators of DN testing in clinical practice (Tang et al. 2021). One study reported that both plasma insulin and GHb were remarkably upregulated in db/db mice (Gould et al. 1986). Our results illustrated that MIC-1 could enhance insulin resistance and decrease the level of GHb in DN mice. Collectively, these findings suggested that MIC-1 can act as an effective therapeutic agent for DN.

The detection of renal pathological morphology can directly indicate the degree of pathological damage of the disease and is a primary indicator for evaluating the therapeutic effect. The histopathological features of DN kidney mainly include glomerular enlargement, mesangial and basement membrane thickening, renal tubular epithelial edema, and inflammatory cell infiltration (Chen et al. 2018). MOS extract has been reported to impede renal tissue damage (Wen et al. 2022). Based on the results of H&E, Masson, and PAS staining of renal tissues, our study proved that MIC-1 could significantly ameliorate the histological damage of glomerulus and renal tubules in DN model rats, indicating that MIC-1 can repair damaged renal tissue and confirm its protective potential on DN renal function at the pathological level.

The pathogenesis of DN is attributed to a multitude of factors such as glucose and lipid metabolism disorders, genetic factors, apoptosis, oxidative stress, and abnormal expression of inflammatory factors, ultimately leading to renal fibrosis (Sagoo and Gnudi 2020; Warren, Knudsen, and Cooper 2019). Among them, apoptosis, inflammatory injury, and oxidative injury are the common pathways involved in and promoting the progression of DN (Turkmen 2017). Epithelial cell apoptosis is the primary feature of early DN, and inhibition of renal tubular epithelial cell apoptosis is particularly considerable for the treatment of DN (Zhang et al. 2014). Bax is a pro-apoptotic

molecule, forming a homologous dimer altering mitochondrial membrane permeability, resulting in increased release of cytochrome C, which further activates the caspase cascade reaction and induces apoptosis (Fu et al. 2020). Conversely, Bcl-2 is an anti-apoptotic molecule, which forms a heterodimer with Bax when its expression increases, weakening the pro-apoptotic effect of Bax (Czabotar et al. 2014). Our study determined apoptosis-related markers in the kidney tissue of DN mice. MIC-1 effectively suppressed apoptosis, as evidenced by increasing Bcl-2 levels and suppressing Bax, cleaved caspase-3, and cleaved caspase-9 levels of kidney tissues in DN mice, unveiling that apoptosis inhibition was one of the mechanisms by which MIC-1 produced anti-DN effects.

Furthermore, the renal inflammatory response and oxidative stress response can stimulate cell proliferation, leading to hyperplasia of mesangial cells and stroma, which is closely associated with the initiation and development of DN (Aghadavod et al. 2016). By detecting the level of MDA, the activities of SOD, CAT, and GPX in the serum of db/db mice, we found that MIC-1 could inhibit oxidative stress in DN mice, thus contributing to its protective function against DN. Moreover, oxidative stress frequently accompanies the inflammatory response, and NLRP3 is an inflammasome widely existing in cells, mainly composed of NLRP3 protein, ASC, and caspase-1 (Jo et al. 2016; Brydges et al. 2013). Activated NLRP3 inflammasome can accelerate the maturation and secretion of various inflammatory factors, and participating in the inflammatory cascade (Kelley et al. 2019). Gao et al. demonstrated that suppression of NLRP3 inflammasome reduced podocyte injury and evidently improved renal tissue injury in DN (Gao et al. 2014). An investigation has reported that MIC-1 inhibited inflammatory factors (IL-6, IL-1β, and TNF-α) in high glucose-mediated human renal proximal tubule cells by activating the Nrf2-ARE pathway (Cheng et al. 2019). This study unveiled that TNF-α, IL-1β, IL-6, NLRP3, ASC, and Caspase-1 expressions were clearly decreased in the kidney tissue homogenate of DN mice by MIC-1 intervention. The above evidence indicated that MIC-1 can weaken the renal inflammatory response and improve the peroxidation state *in vivo*, thereby mitigating the severity of renal tissue injury and playing a protective role in the kidney.

In conclusion, MIC-1 notably improve the kidney injury of DN mice, and its mechanism might be correlated with the decrease in renal cell apoptosis, oxidative stress, and inflammatory responses. This finding provides a clue for studying the specific molecular mechanism of DN, which will be

verified in primary renal tubular epithelial cells in further research.

Declarations

Ethics statement

All animal protocols were performed in compliance with the Institutional Animal Care and Use Committee. Ethical approval for animal manipulations was granted by the Ethics Committee of Zhejiang Eyong Biotechnological Co., Ltd. We spared no effort to lighten the suffering of animals during the experiments.

Conflict of Interests

The authors report there are no competing interests to declare.

Acknowledgments

Not applicable.

Figure legends

Figure 1. MIC-1 attenuated the renal impairment of db/db mice **(A)** The schematic representation of the animal model. **(B)** The body weight, kidney weight, kidney/body weight ratio of mice**,** fasting blood Glu, serum creatinine, and urine albumin in each group were assessed (n=6). Quantitative data were described as mean ± standard deviation. $^{**}P$<0.01 vs. db/m; $^{\#}P$<0.05, $^{\#\#}P$<0.01 vs. db/db. In the db/m group, C57BLKS/J-db/m mice were used as a control. The C57BLKS/J-db/db mice in the db/db + irbesartan (IBS) group were subjected to IBS at a dose of 50 mg/kg/d for 21 days. The db/db mice in the db/db + moringa isothiocyanate-1 (MIC-1) group were treated with MIC-1 at a dose of 100 mg/kg/d for 21 days.

Figure 2. MIC-1 suppressed oxidative stress of db/db mice Corresponding kits were utilized to examine the levels of malondialdehyde (MDA) **(A)**, activities of superoxide dismutase (SOD) **(B)**, catalase (CAT) **(C)**, and glutathione peroxidase (GPX) **(D)** in the serum of db/db and db/m mice (n=6). Quantitative data were expressed as mean ± standard deviation. $^{**}P$<0.01 vs. db/m; $^{\#\#}P$<0.01 vs. db/db

Figure 3. MIC-1 mitigated the kidney tissue injury of db/db mice The kidney tissue injury of db/db mice was assessed by Hematoxylin & Eosin (H&E), Masson, and Periodic Acid-Schiff (PAS) staining (x 400).

Figure 4. The insulin and GHb contents in db/db mice were decreased by MIC-1 treatment in db/db mice **(A)** Serum insulin was assessed utilizing the Mouse Ins1 / Insulin-1 ELISA Kit (n=6). **(B)** The level of glycosylated hemoglobin (GHb) was estimated utilizing an automated GHb analyzer (n=6). Quantitative data were described as mean ± standard deviation. $^{**}P$<0.01 vs. db/m; $^{\#\#}P$<0.01 vs. db/db

Figure 5. MIC-1 inhibited the apoptosis of db/db mice **(A)** TUNEL staining was used to assess the apoptosis of the kidney tissues (n=6). **(B)** The protein levels of Bcl-2, Bax, cleaved caspase-3, caspase-3, caspase-9, and cleaved caspase-9 in the kidney tissues of each group were assessed by Western blot (n=3). Quantitative data were manifested as mean ± standard deviation. $^{**}P$<0.01 vs.

db/m; $^{\#}P<0.05$, $^{\#\#}P<0.01$ vs. db/db

Figure 6. MIC-1 alleviated the inflammatory response of db/db mice The tumor necrosis factor-α (TNF-α) **(A)**, interleukin-1β (IL-1β) **(B)**, and IL-6 **(C)** levels of the serum in each group were assessed by the corresponding kits (n=6). Quantitative data were described as mean ± standard deviation. $^{**}P<0.01$ vs. db/m; $^{\#\#}P<0.01$ vs. db/db

Figure 7. MIC-1 suppressed NLRP3, ASC, and caspase-1 levels of the kidney tissues in db/db mice **(A-B)** The NOD-like receptor family pyrin domain containing 3 (NLRP3), apoptosis-associated speck-like protein containing a caspase recruitment domain (ASC), pro-caspase-1, and caspase-1 levels of the kidney tissues in db/db mice were examined utilizing Western blot (n=3). Quantitative data were presented as mean ± standard deviation. $^{**}P<0.01$ vs. db/m; $^{\#}P<0.05$, $^{\#\#}P<0.01$ vs. db/db

References

Aghadavod E., Khodadadi S., Baradaran A., Nasri P., Bahmani M. and Rafieian-Kopaei M. (2016). Role of oxidative stress and inflammatory factors in diabetic kidney disease. *Iran J. Kidney Dis*. 10, 337-343.

Araújo L.C.C., Aguiar J.S., Napoleão T.H., Mota F.V., Barros A.L., Moura M.C., Coriolano M.C., Coelho L.C.B.B., Silva T.G. and Paiva P.M. (2013). Evaluation of cytotoxic and anti-inflammatory activities of extracts and lectins from Moringa oleifera seeds. *PLoS One* 8, e81973.

Brydges S.D., Broderick L., McGeough M.D., Pena C.A., Mueller J.L. and Hoffman H.M. (2013). Divergence of IL-1, IL-18, and cell death in NLRP3 inflammasomopathies. *J. Clin. Invest*. 123, 4695-705.

Chen J., Ren J., Loo W.T.Y., Hao L. and Wang M. (2018). Lysyl oxidases expression and histopathological changes of the diabetic rat nephron. *Mol. Med. Rep*. 17, 2431-2441.

Cheng D., Gao L., Su S., Sargsyan D., Wu R., Raskin I. and Kong A.N. (2019). Moringa Isothiocyanate Activates Nrf2: Potential role in diabetic nephropathy. *AAPS J*. 21, 31.

Czabotar P.E., Lessene G., Strasser A. and Adams J.M. (2014). Control of apoptosis by the BCL-2 protein family: implications for physiology and therapy. *Nat. Rev. Mol. Cell Biol*. 15, 49-63.

Deng X., Cheng J. and Shen M. (2016). Vitamin D improves diabetic nephropathy in rats by inhibiting renin and relieving oxidative stress. *J. endocrinol. invest*. 39, 657-666.

Fakurazi S., Hairuszah I. and Nanthini U. (2008). Moringa oleifera Lam prevents acetaminophen induced liver injury through restoration of glutathione level. *Food Chem. Toxicol*. 46, 2611-2615.

Fu D.L., Jiang H., Li C.Y., Gao T., Liu M.R. and Li. H.W. (2020). MicroRNA-338 in MSCs-derived exosomes inhibits cardiomyocyte apoptosis in myocardial infarction. *Eur. Rev. Med. Pharmacol. Sci*. 24, 10107-10117.

Gao P., Meng X.F., Su H., He F.F., Chen S., Tang H., Tian X.J., Fan D., Y. Wang Y.M., Liu J.S., Zhu Z.H. and

Zhang C. (2014). Thioredoxin-interacting protein mediates NALP3 inflammasome activation in podocytes during diabetic nephropathy. *Biochim. Biophys. Acta* 1843, 2448-2460.

Giacoppo S., Rajan T.S., Iori R., Rollin P., Bramanti P. and Mazzon E. (2017). The α-cyclodextrin complex of the Moringa isothiocyanate suppresses lipopolysaccharide-induced inflammation in RAW 264.7 macrophage cells through Akt and p38 inhibition. *Inflamm. Res.* 66, 487-503.

Gould B.J., Flatt P.R., Kotecha S., Collett S. and Swanston-Flatt S.K. (1986). Measurement of glycosylated haemoglobins and glycosylated plasma proteins in animal models with diabetes or inappropriate hypoglycaemia. *Horm. Metab. Res*. 18, 795-799.

Ioannou K. (2017). Diabetic nephropathy: is it always there? Assumptions, weaknesses and pitfalls in the diagnosis. *Hormones (Athens)*. 16, 351-361.

Jin Y.H., Li Z.T., Chen H., Jiang X.Q., Zhang Y.Y. and Wu F. (2019). Effect of dexmedetomidine on kidney injury in sepsis rats through TLR4/MyD88/NF-κB/iNOS signaling pathway. *Eur. Rev. Med. Pharmacol. Sci*. 23, 5020-5025.

Jo E.K., Kim J.K., Shin D.M. and Sasakawa C. (2016). Molecular mechanisms regulating NLRP3 inflammasome activation. *Cell. Mol. Immunol*. 13, 148-159.

Kelley N., Jeltema D., Duan Y. and He Y. (2019). The NLRP3 Inflammasome: An Overview of Mechanisms of Activation and Regulation. *Int. J. Mol. Sci*. 20, 3328.

Kim Y., Wu A.G., Jaja-Chimedza A., Graf B.L., Waterman C., Verzi M.P. and Raskin I. (2017). Isothiocyanate-enriched moringa seed extract alleviates ulcerative colitis symptoms in mice. *PLoS One* 12, e0184709.

Kim Y., Jaja-Chimedza A., Merrill D., Mendes O. and Raskin I. (2018). A 14-day repeated-dose oral toxicological evaluation of an isothiocyanate-enriched hydro-alcoholic extract from *Moringa oleifera* Lam. seeds in rats. *Toxicol. Rep*. 5, 418-426.

Kou X., B. Li, Olayanju J.B., Drake J.M. and Chen N. (2018). Nutraceutical or pharmacological potential of Moringa oleifera Lam. *Nutrients* 10, 343.

Li S., Li W., Wu R., Yin R., Sargsyan D., Raskin I. and Kong A.N. 2019. 'Epigenome and transcriptome study of moringa isothiocyanate in mouse kidney mesangial cells induced by high glucose, a potential model for diabetic-induced nephropathy. *AAPS J*. 22, 8.

Ma L., Wu F., Shao Q., Chen G., Xu L. and Lu F. (2021). Baicalin alleviates oxidative stress and Inflammation in Diabetic Nephropathy via Nrf2 and MAPK Signaling Pathway. *Drug Des. Devel. Ther*. 15, 3207-3221.

Ou Y., Zhang W., Chen S. and Deng H. (2021). Baicalin improves podocyte injury in rats with diabetic nephropathy by inhibiting PI3K/Akt/mTOR signaling pathway. *Open Med (Wars)* 16, 1286-1298.

Padla E.P., Solis L.T., Levida R.M., Shen C.C. and Ragasa C.Y. (2012). Antimicrobial isothiocyanates from the seeds of Moringa oleifera Lam. *Z Naturforsch C J. Biosci*. 67, 557-564.

Sagoo M.K. and Gnudi L. (2020). Diabetic nephropathy: An Overview. *Methods Mol. Biol*. 2067, 3-7.

Sailaja B.S., Aita R., Maledatu S., Ribnicky D., Verzi M.P. and Raskin I. (2021). Moringa isothiocyanate-1 regulates Nrf2 and NF-κB pathway in response to LPS-driven sepsis and inflammation. *PLoS One* 16, e0248691.

Samsu N. (2021). Diabetic nephropathy: Challenges in pathogenesis, diagnosis, and treatment. *Biomed. Res. Int*. 2021, 1497449.

Tang S.C. W. and Yiu W.H. (2020). Innate immunity in diabetic kidney disease. *Nat. Rev. Nephrol*. 16, 206-222.

Tang G., Li S., Zhang C., Chen H., Wang N. and Feng Y. (2021). Clinical efficacies, underlying mechanisms

and molecular targets of Chinese medicines for diabetic nephropathy treatment and management. *Acta Pharm. Sin. B* 11, 2749-2767.

Turkmen K. (2017). Inflammation, oxidative stress, apoptosis, and autophagy in diabetes mellitus and diabetic kidney disease: the Four Horsemen of the Apocalypse. *Int. Urol. Nephrol*. 49, 837-844.

Vasanth Rao V.R.A/L.B., Tan S.H., Candasamy M. and Bhattamisra S.K. (2019). Diabetic nephropathy: An update on pathogenesis and drug development. *Diabetes Metab. Syndr*. 13, 754-762.

Warren A.M., Knudsen S.T. and Cooper M.E. (2019). Diabetic nephropathy: an insight into molecular mechanisms and emerging therapies. *Expert Opin. Ther. Targets* 23, 579-591.

Waterman C., Graham J.L., Arnold C.D., Stanhope K.L., Tong J.H., Jaja-Chimedza A. and Havel P.J. (2020). Moringa isothiocyanate-rich seed extract delays the onset of diabetes in UC davis type-2 diabetes mellitus rats. *Sci. Rep*. 10, 8861.

Wen Y., Liu Y., Huang Q., Liu R., Liu J., Zhang F., Liu S. and Jiang Y. (2022). Moringa oleifera Lam. seed extract protects kidney function in rats with diabetic nephropathy by increasing GSK-3β activity and activating the Nrf2/HO-1 pathway. *Phytomedicine* 95, 153856.

Xie J., Qian Y.Y., Yang Y., Peng L.J., Mao J.Y., Yang M.R., Tian Y. and Sheng J. (2021). Isothiocyanate From *Moringa* oleifera Seeds Inhibits the Growth and Migration of Renal Cancer Cells by Regulating the PTP1B-dependent Src/Ras/Raf/ERK Signaling Pathway. *Front. Cell Dev. Biol*. 9. 790618.

Yamazaki T., Mimura I., Tanaka T. and Nangaku M. (2021). Treatment of diabetic kidney disease: Current and future. *Diabetes Metab. J*. 45, 11-26.

Zhang X., Zhao Y., Chu Q., Wang Z.Y., Li H. and Chi Z.H. (2014). Zinc modulates high glucose-induced apoptosis by suppressing oxidative stress in renal tubular epithelial cells. *Biol. Trace Elem. Res*. 158, 259-267.

A

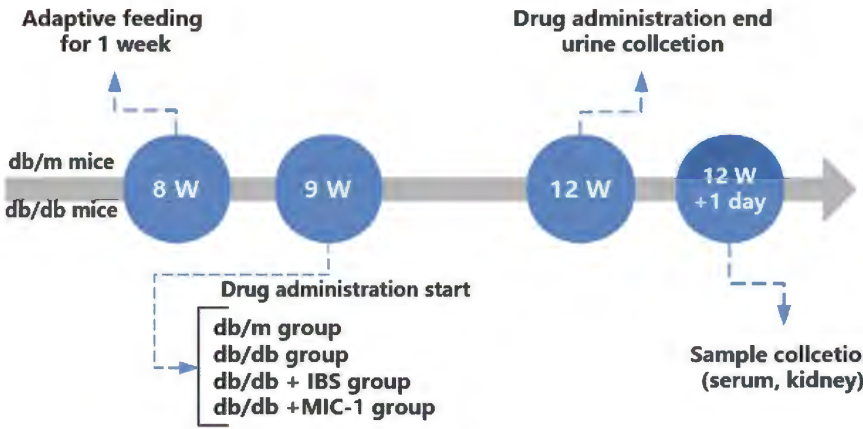
Adaptive feeding
for 1 week
Drug administration end
urine collcetion
db/m mice
db/db mice
8 W
9 W
12 W
12 W
+1 day
Drug administration start
db/m group
db/db group
db/db + IBS group
db/db +MIC-1 group
Sample collcetion
(serum, kidney)

B

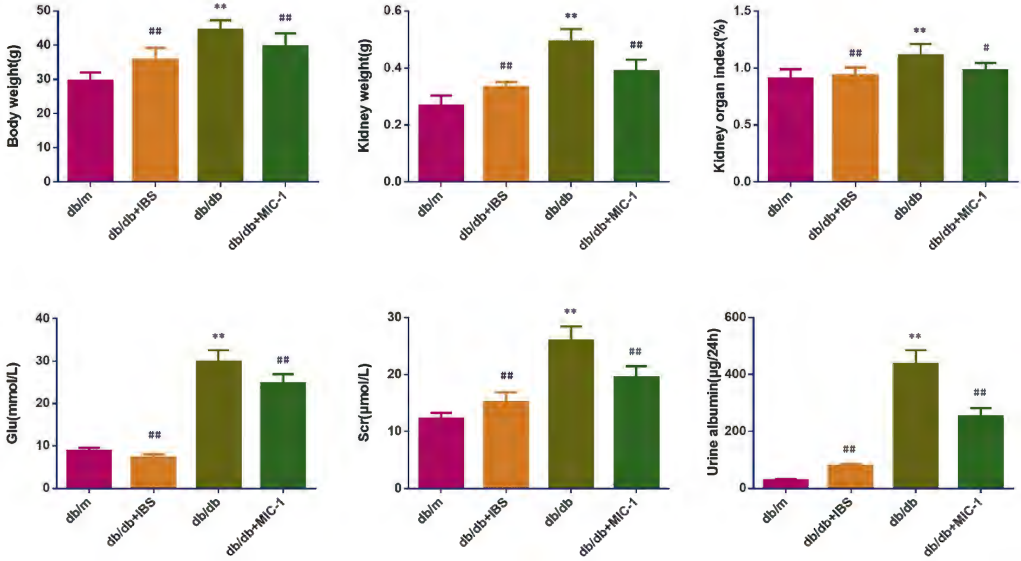
Body weight(g)
Kidney weight(g)
Kidney organ index(%)
Glu(mmol/L)
Scr(μmol/L)
Urine albumin(μg/24h)
db/m
db/db+IBS
db/db
db/db+MIC-1

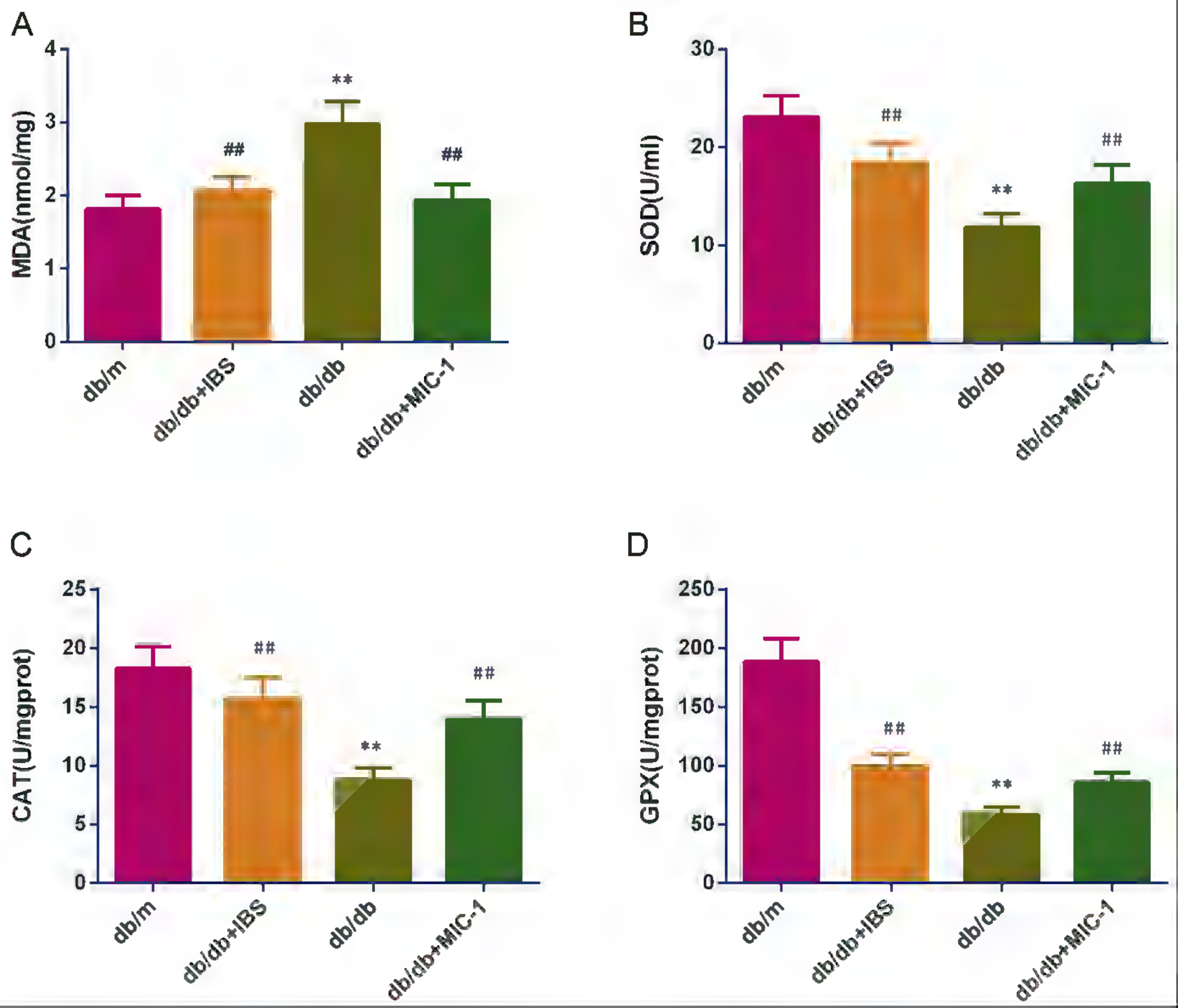
A
MDA(nmol/mg)
4
3
2
1
0
**
##
##
db/m
db/db+IBS
db/db
db/db+MIC-1
B
SOD(U/ml)
30
20
10
0
##
**
##
db/m
db/db+IBS
db/db
db/db+MIC-1
C
CAT(U/mgprot)
25
20
15
10
5
0
##
**
##
db/m
db/db+IBS
db/db
db/db+MIC-1
D
GPX(U/mgprot)
250
200
150
100
50
0
##
**
##
db/m
db/db+IBS
db/db
db/db+MIC-1

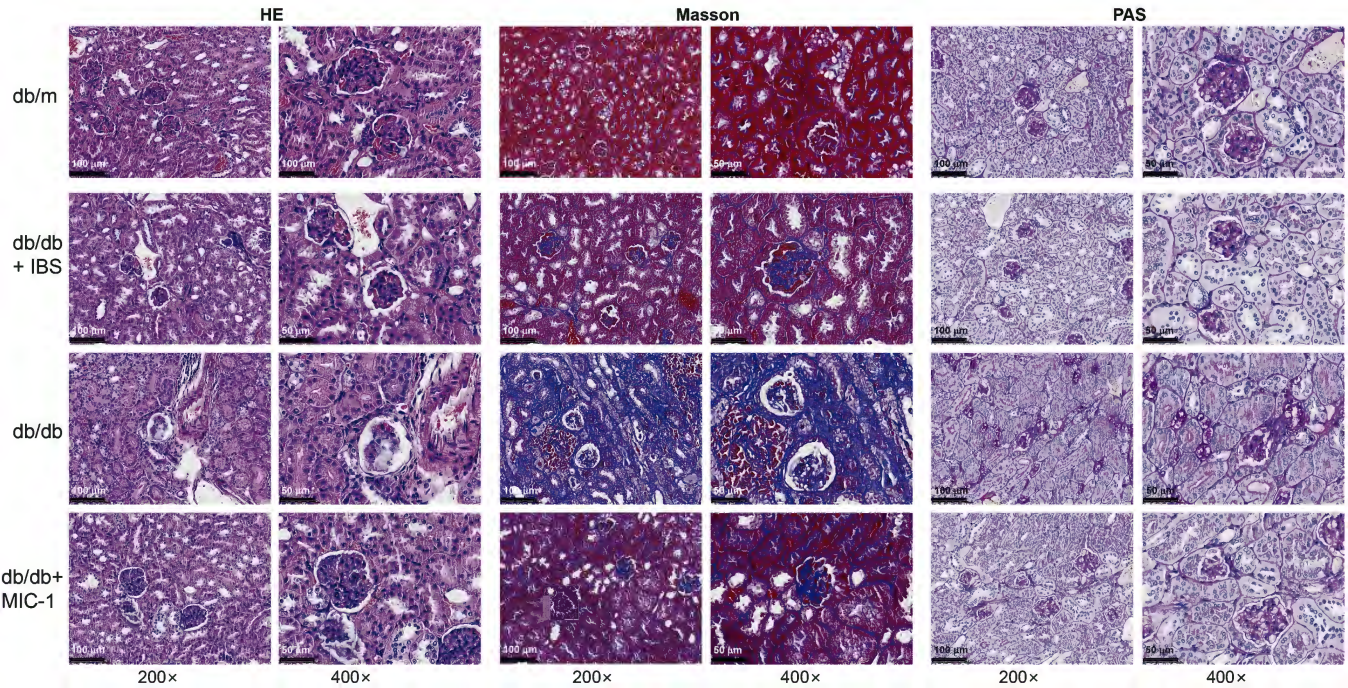
HE
Masson
PAS
db/m
db/db
+ IBS
db/db
db/db+
MIC-1
100 μm
50 μm
200×
400×
200×
400×
200×
400×

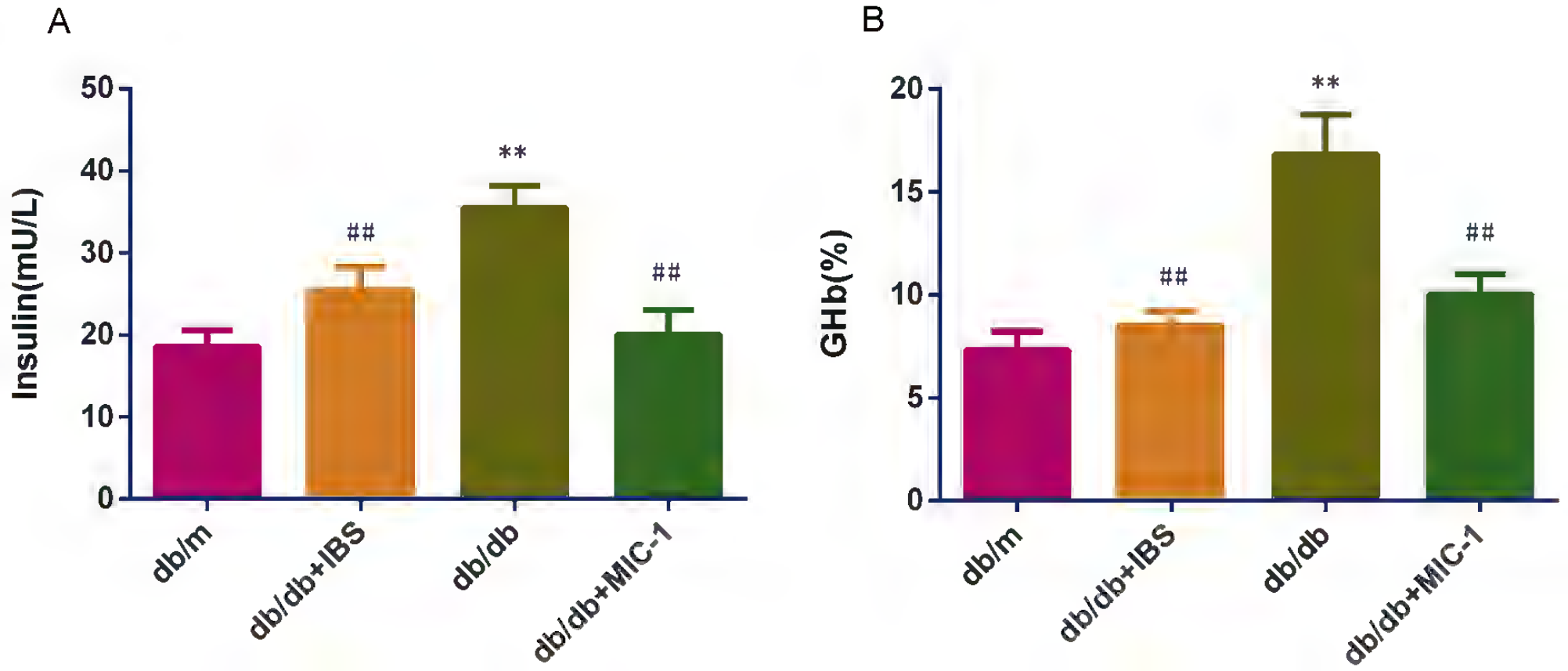
A
Insulin(mU/L)
50
40
30
20
10
0
**
##
##
db/m
db/db+IBS
db/db
db/db+MIC-1
B
GHb(%)
20
15
10
5
0
**
##
##
db/m
db/db+IBS
db/db
db/db+MIC-1

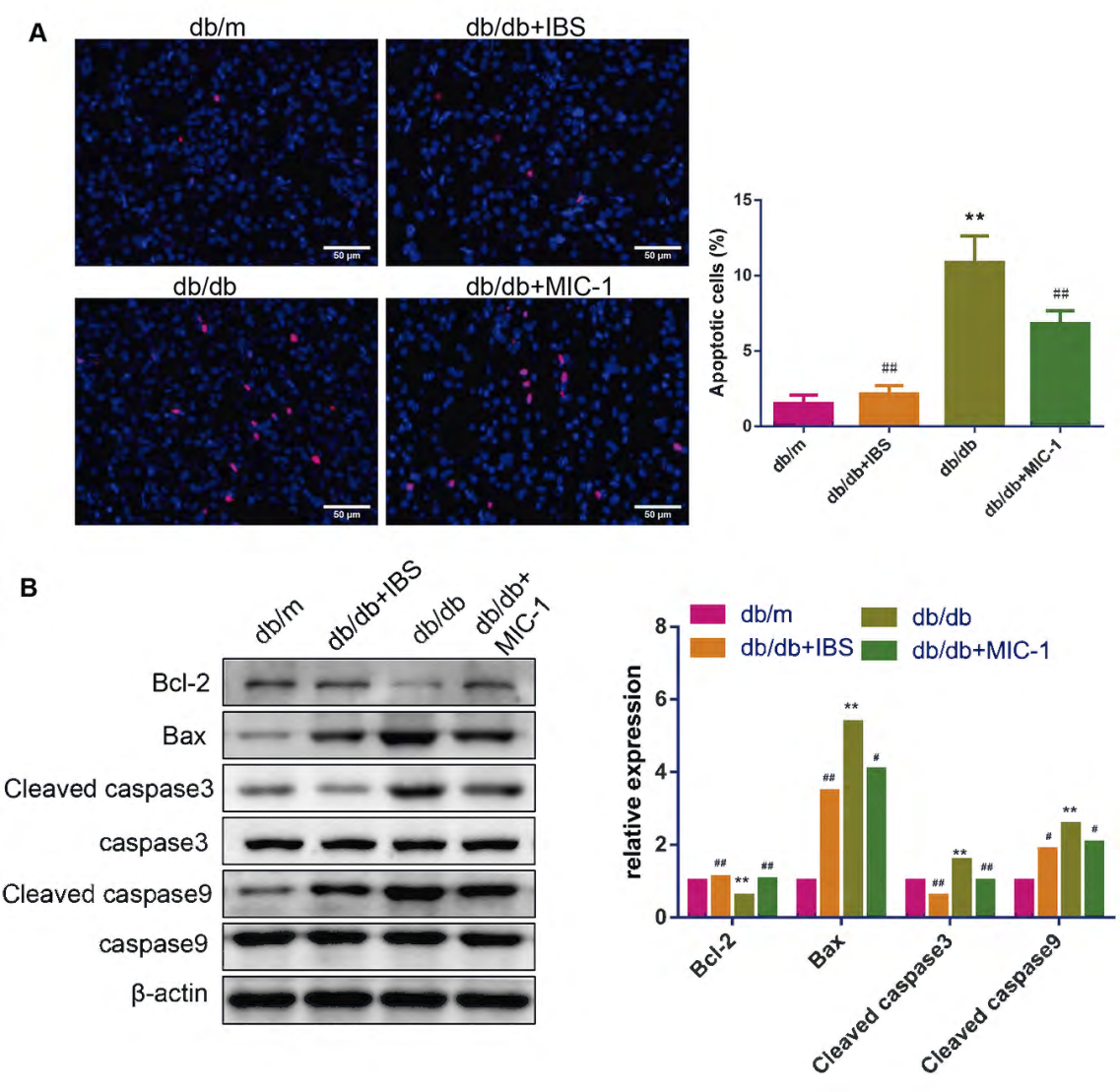
A
db/m
db/db+IBS
db/db
db/db+MIC-1
50 μm
Apoptotic cells (%)
15
10
5
0
**
##
db/m
db/db+IBS
db/db
db/db+MIC-1
B
db/m
db/db+IBS
db/db
db/db+ MIC-1
Bcl-2
Bax
Cleaved caspase3
caspase3
Cleaved caspase9
caspase9
β-actin
relative expression
8
6
4
2
0
Bcl-2
Bax
Cleaved caspase3
Cleaved caspase9

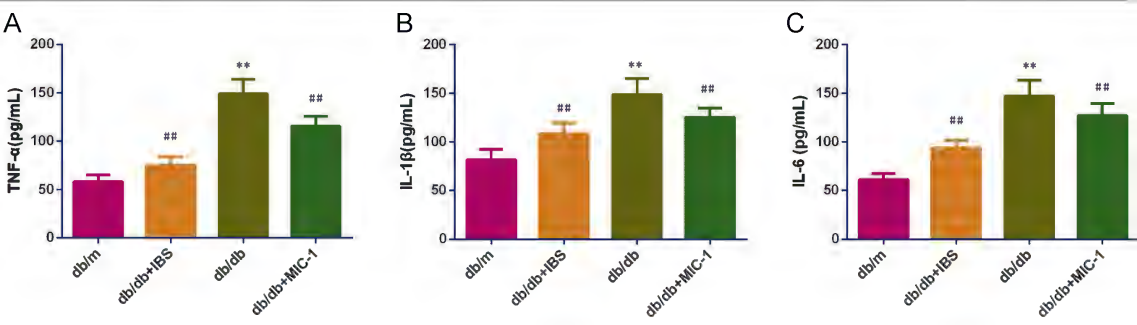
A
TNF-α(pg/mL)
200
150
100
50
0
##
**
##
db/m
db/db+IBS
db/db
db/db+MIC-1
B
IL-1β(pg/mL)
200
150
100
50
0
##
**
##
db/m
db/db+IBS
db/db
db/db+MIC-1
C
IL-6 (pg/mL)
200
150
100
50
0
##
**
##
db/m
db/db+IBS
db/db
db/db+MIC-1

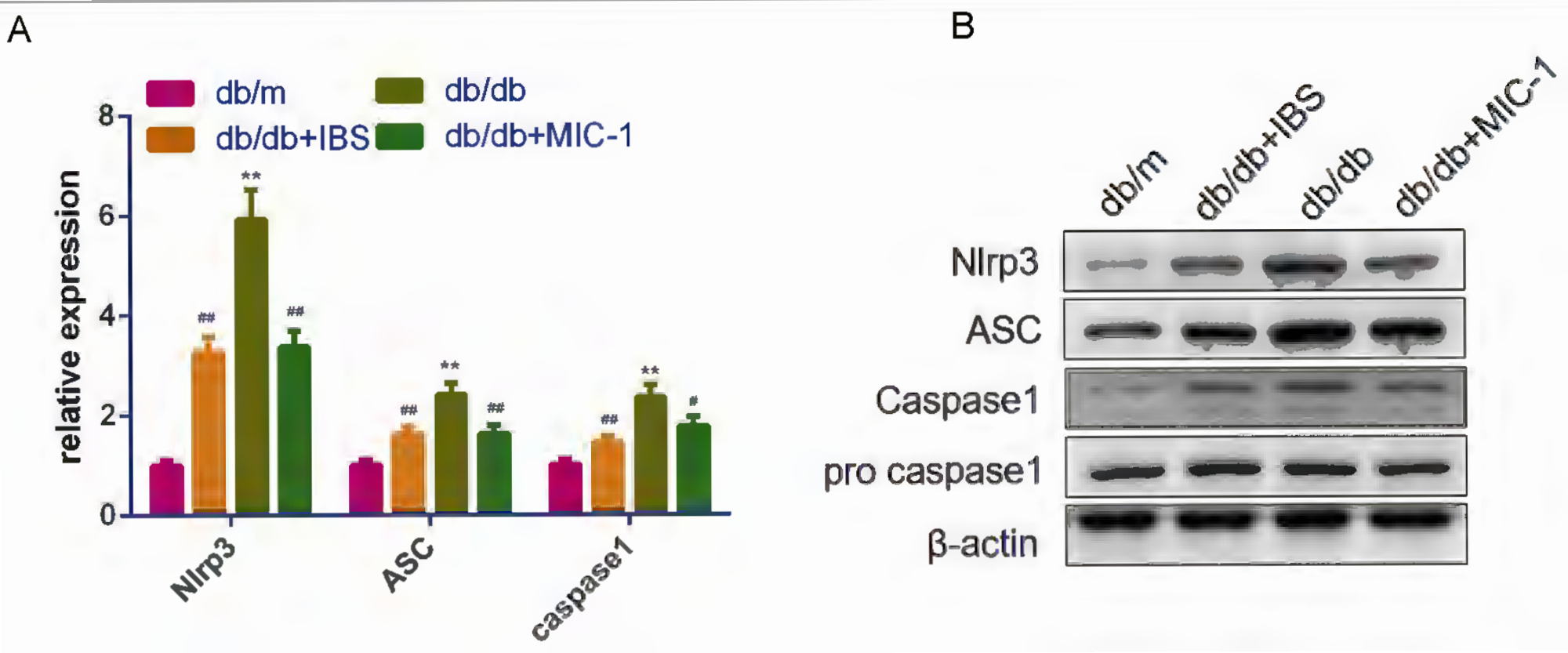
A
db/m
db/db
db/db+IBS
db/db+MIC-1
relative expression
8
6
4
2
0
**
##
Nlrp3
ASC
caspase1
B
db/m
db/db+IBS
db/db
db/db+MIC-1
Nlrp3
ASC
Caspase1
pro caspase1
β-actin